A Learning-Based Approach for Traffic State Reconstruction from Limited Data

Nail Baloul, Amaury Hayat, Thibault Liard, Pierre Lissy [1]

2025 IEEE 64th Conference on Decision and Control (CDC), Rio de Janeiro

December, 12th 2025

ÉCOLE NATIONALE DES PONTS ET CHAUSSÉES

IP PARIS

[1] N. Baloul, A. Hayat, and P. Lissy are with CERMICS, ENPC and T. Liard is with XLIM, Université de Limoges

Outline

Introduction

State-of-the art traffic flow models

(Learning-based) Optimization for traffic flow reconstruction

Numerical experiments

Conclusion and perspectives

Table of contents

Introduction

State-of-the art traffic flow models

(Learning-based) Optimization for traffic flow reconstruction

Numerical experiments

Conclusion and perspectives

Motivation

Traffic jam in Rio de Janeiro

- Traffic management relies on **control** schemes to address perturbed traffic conditions
- Most existing control techniques require complete and accurate knowledge of state
- In practice, full information is rarely available due to limited and noisy measurements
- **Goal** $\Rightarrow$ develop reliable methods for **estimating traffic from partial data**

Microscopic model

- Microscopic scale $\Rightarrow$ individual vehicle dynamics, full trajectory information
- Tracks position $x_i(t)$, velocity $v_i(t)$ of vehicle i at time t
- Each driver responds to surrounding traffic by adjusting speed

$$\begin{aligned} \dot{x}_i(t) &= v_i(t) \\ \dot{v}_i(t) &= F(v_i(t), \Delta x_i(t), \Delta v_i(t)) \end{aligned} \tag{1}$$

- Agent-based simulation capturing detailed vehicle dynamics and interactions

Macroscopic model

- Macroscopic scale $\Rightarrow$ traffic as continuous fluid
- Describes aggregated variables: density $\rho(t,x)$, velocity $v(\rho)$, flux $f(\rho)$
- Total number of cars is conserved via continuity

$$0 = f(\rho(t,a)) - f(\rho(t,b)) = \frac{d}{dt}\int_a^b \rho(t,x)dx \tag{2}$$

- Fundamental diagram relates flow-density: $f(\rho) = \rho v_{\mathrm{eq}}(\rho)$

Table of contents

Introduction

State-of-the art traffic flow models

(Learning-based) Optimization for traffic flow reconstruction

Numerical experiments

Conclusion and perspectives

Model-based approaches

- Follow-the-Leader (FtL), **microscopic** first order model
  $\Rightarrow$ dynamics of each vehicle depend on vehicle immediately in front

$$\begin{cases} \dot{x}_N^N(t) = v_{\max}, & t > 0, \\ \dot{x}_i^N(t) = v\left(\frac{L}{N(x_{i+1}^N(t) - x_i^N(t))}\right), & t > 0, \quad i = 0, \cdots, N-1 \\ x_i^N(0) = \bar{x}_i^N, & i = 0, \cdots, N \end{cases} \tag{3}$$

  $\Rightarrow$ accurate traffic representation, encodes individual movements
  $\Rightarrow$ computationally demanding, requires more data
  $\Rightarrow$ involves solving large systems of coupled nonlinear ODE sensitive to initial conditions

Model-based approaches

- Lighthill-William-Richards (LWR), **macroscopic** traffic flow model
  $\Rightarrow$ vehicles treated as a continuous medium: one-dimensional (hyperbolic) conservation law

$$\begin{cases} \partial_t \rho(t,x) + \partial_x f(\rho(t,x)) = 0, & x \in \mathbb{R}, \quad t > 0, \\ \rho(0,x) = \bar{\rho}(x), & x \in \mathbb{R} \end{cases} \tag{4}$$

  $\Rightarrow$ faster implementation, less data-intensive
  $\Rightarrow$ overlooks traffic heterogeneity, oversimplifies traffic phenomena
  $\Rightarrow$ PDE analysis requires advanced techniques to handle discontinuities

Model-based approaches

- **Convergence analysis of FtL approximation scheme towards LWR model**[2]

  $\Rightarrow$ link between FtL and LWR based on atomization of initial density $\bar{\rho}$

$$\bar{x}_{i+1}^N := \sup\left\{x \in \mathbb{R} : \int_{\bar{x}_i^N}^{x} \bar{\rho}(y)dy = \frac{L}{N}\right\}, \quad i = 0, \cdots, N-1 \tag{5}$$

  $\Rightarrow$ solution of PDE (3) can be recovered as many particle limit[3] of ODE system (4)

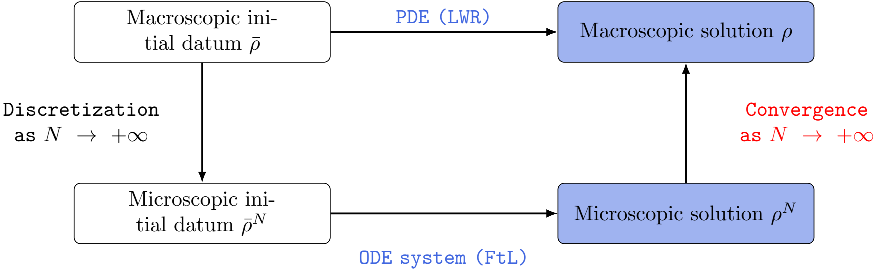

Coupled resolution of a microscopic ODE system and a macroscopic PDE

[2] Holden and Risebro 2017.

[3] Di Francesco and Rosini 2015.

- Hybrid micro-macro models explored in traffic density reconstruction[4]

$$\begin{cases} \dot{x}_N^N(t) = v_{\max}, & t > 0, \\ \dot{x}_i^N(t) = v\left(\rho(t, x_i^N(t))\right), & t > 0, \quad i = 0, \cdots, N-1 \\ \partial_t \rho(t,x) + \partial_x f(\rho(t,x)) = \gamma^2 \partial_{x,x} \rho(t,x), & x \in \mathbb{R}, \quad t > 0, \end{cases} \tag{6}$$

where $\gamma^2 \partial_{x,x}$ is a diffusion correction term to handle discontinuous solutions of original PDE

$\Rightarrow$ **partial state reconstruction**[5] using measurements from low penetration rate: $N_{\text{probes}} \ll N_{\text{total}}$

$\Rightarrow$ requires access to real-time positions, densities and instantaneous speeds of PVs

$\Rightarrow$ no guarantee of convergence of reconstructed density to imposed conservation law

[4] Barreau, Aguiar, Liu, and Johansson 2021.

[5] Liu, Barreau, Cicic, and Johansson 2020.

Table of contents

Introduction

State-of-the art traffic flow models

(Learning-based) Optimization for traffic flow reconstruction

Numerical experiments

Conclusion and perspectives

Parametrized microscopic model

- **Limited data scenario** $\Rightarrow$ only **initial and final** $\left\{\left(\bar{x}_i^N, \bar{y}_i^N\right)\right\}_{i=0}^n$ positions of **PVs**
- **Enhanced** version of FtL (3): α^N accounts for unobserved vehicles between consecutive PVs
- Parametrized ODE system with **finite time horizon**

$$\begin{cases} \dot{x}_n^N(t) = v_{\max}, & t \in (0, T] \\ \dot{x}_i^N(t) = v\left(\rho_i^N(t)\right), & t \in (0, T] \quad i = 0, \cdots, n-1 \\ x_i^N(0) = \bar{x}_i^N, & i = 0, \cdots, n \end{cases} \tag{7}$$

$\Rightarrow$ local discrete densities

$$\rho_i^N(t) := \frac{\alpha_i^N L}{N\left(x_{i+1}^N(t) - x_i^N(t)\right)}, \quad t \in (0, T], \quad i = 0, \cdots, n-1 \tag{8}$$

- Piecewise constant Eulerian discrete density

$$\rho^N(t, x) := \sum_{i=0}^{N-1} \rho_i^N(t)\chi_{[x_i^N(t), x_{i+1}^N(t))}(x), \quad x \in \mathbb{R}, \quad t \in [0, T] \tag{9}$$

Well-posedness

- Assumptions on velocity

$$v \in C^1([0,+\infty)) \tag{10a}$$
$$v \text{ is decreasing on } [0,+\infty) \tag{10b}$$
$$v(0) = v_{\max} < \infty \tag{10c}$$

- Local existence and uniqueness of solution to (7) (for fixed α) via Picard-Lindelöf
- Condition on initial car positions $\bar{x}_0^N < \bar{x}_1^N < \cdots < \bar{x}_{n-1}^N < \bar{x}_n^N$
  $\Rightarrow$ global existence

Lemma (Discrete maximum principle)

For solution $x(t)$ of (7) with v satisfying (10a)-(10c), for all $i = 0, \cdots, n-1$,

$$\frac{\alpha_i^N L}{NM} \le x_{i+1}^N(t) - x_i^N(t) \le \bar{x}_n^N - \bar{x}_0^N + (v_{\max} - v(M))\, t, \quad \forall t \in [0,T], \tag{11}$$

where $M := \max_i \left(\frac{\alpha_i^N L}{N(\bar{x}_{i+1}^N - \bar{x}_i^N)} \right)$

ODE-constrained optimization

- Physical conditions on $\alpha := \alpha^N$ induce feasible set

$$\mathcal{A}^N := \left\{ \alpha \in \mathbb{R}^n : \quad \alpha_i \in \left[1, \bar{z}_i^N\right], \quad i = 0, \dots, n-1, \quad \sum_{i=0}^{n-1} \alpha_i = N \right\} \tag{12}$$

with $\bar{z}_i^N := \min \left\{ \frac{N\left(\bar{x}_{i+1}^N - \bar{x}_i^N\right)}{L}, \frac{N\left(\bar{y}_{i+1}^N - \bar{y}_i^N\right)}{L} \right\}, \quad i = 0, \dots, n-1$

- **Approximate density reconstruction** $\Rightarrow$ find optimal interaction parameter α

$$\begin{aligned} \underset{\alpha}{\text{minimize}} \quad & \frac{1}{2} \left\| x(T) - \bar{y} \right\|^2 \\ \text{s.t.} \quad & \dot{x}(t) = V\left(W_\alpha x(t) + b_\alpha(t)\right) \\ & x(0) = \bar{x} \\ & \alpha \in \mathcal{A}^N \end{aligned} \tag{13}$$

- Existence of solutions guaranteed by continuity of $V := v \circ \frac{1}{\cdot}$ and compactness of $\mathcal{A}^N$
- No uniqueness (a priori) since nonlinear dynamics can lead to multiple minima

ResNet Learning Architecture

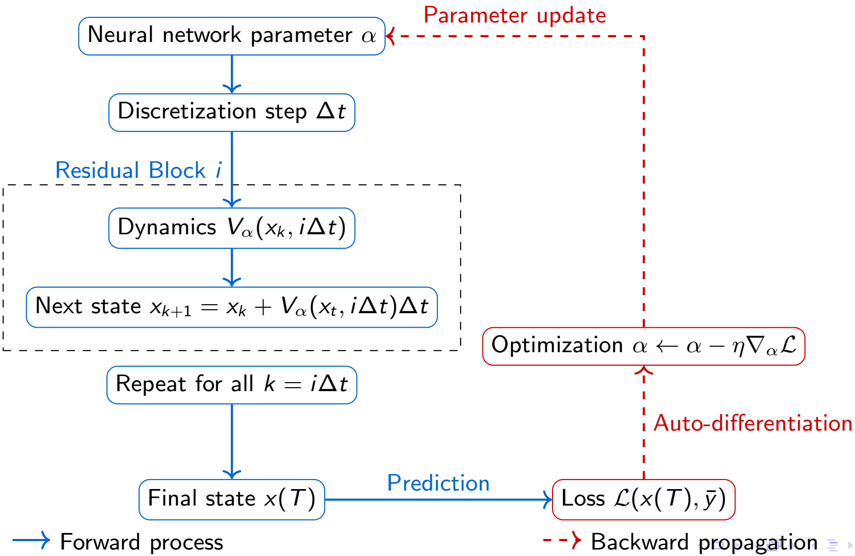

Model validation

- Through predicted parameter $\bar{\alpha}$, training yields piecewise constant discrete density

$$\rho^N(t,x) = \sum_{i=0}^{n-1} \frac{\bar{\alpha}_i L}{N(x_{i+1}^N(t) - x_i^N(t))} \chi_{[x_i^N(t), x_{i+1}^N(t))}(x), \quad x \in \mathbb{R}, \quad t \in [0,T], \tag{14}$$

- Simulation on **test data** by solving ODE system

$$\begin{cases} \dot{x}_i^N(t) = v\left(\rho^N(t, x_i(t)^+)\right), & t \in (0,T], \\ x_i^N(0) = \bar{x}_i^N & i = 0, \dots, n_{\text{test}} \end{cases} \tag{15}$$

- Assess model's performance by measuring test error $L^{\text{test}}(x(T), \bar{y}) = \frac{1}{n_{\text{test}}} \sum_{j=0}^{n_{\text{test}}} |x_j^{\bar{\alpha}}(T) - \bar{y}_i^N|^2$

Theorem Convergence of approximate density to solution of LWR

Assuming the controlled–growth condition

$$\max_{i=0,\dots,n-1} \alpha_i^N = o(N). \tag{16}$$

$$\rho^N(t,x) = \sum_{i=0}^{n-1} \frac{\bar{\alpha}_i^N L}{N(x_{i+1}^N(t) - x_i^N(t))} \chi_{[x_i^N(t), x_{i+1}^N(t))}(x), \quad x \in \mathbb{R}, \quad t \in [0, T], \tag{17}$$

where $\bar{\alpha}_i^N \in \mathcal{A}^N$ is a solution to (13) converges to **unique solution** ρ of

$$\begin{cases} \partial_t \rho(t,x) + \partial_x f(\rho(t,x)) = 0, \quad x \in \mathbb{R}, \quad t \in [0, T], \\ \rho(0,x) = \bar{\rho}(x), \quad x \in \mathbb{R} \end{cases} \tag{18}$$

which satisfies **Kruzhkov entropy condition**

$$\int_0^T \int_{\mathbb{R}} |u - k| \frac{\partial \phi}{\partial t} + \mathrm{sign}(u-k)(f(u) - f(k)) \frac{\partial \phi}{\partial x} dxdt \geq 0, \quad \forall k \in \mathbb{R} \tag{19}$$

Table of contents

Introduction

State-of-the art traffic flow models

(Learning-based) Optimization for traffic flow reconstruction

Numerical experiments

Conclusion and perspectives

Numerical experiments

- Parameters
  - Maximum traffic speed $v_{\max} = 120$ km/h
  - Maximum traffic density $\rho_{\max} = 200$ cars/km
  - Greenshields velocity $v(\rho) = v_{\max} \max\left\{1 - \frac{\rho}{\rho_{max}}, 0\right\}, \quad \rho \in [0, \rho_{max}]$
  - Final time horizon $T = 0.05$ h or $T = 0.15$ h
- Sampling such 10% **of total fleet serve as PVs for training and** 2.5% **for testing**
- **Stop-and-go wave** characterized by **alternating regions of congestion and free flow**

Stop-and-go wave scenario

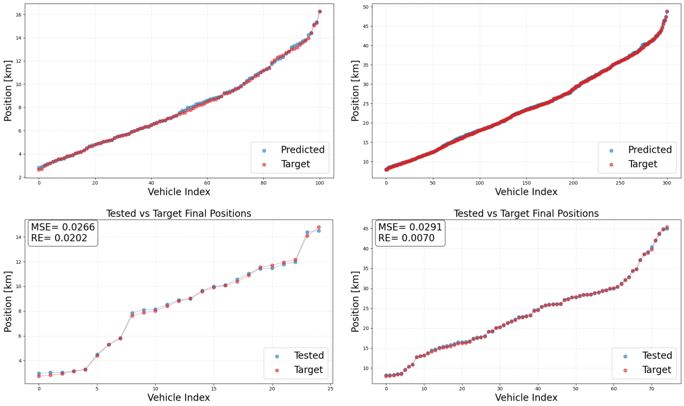

(a) $N = 1000$ (b) $N = 3000$

Comparison of predicted and target final PV positions: **Top** Results from **training** procedure, **Bottom** Results on **test** sounds

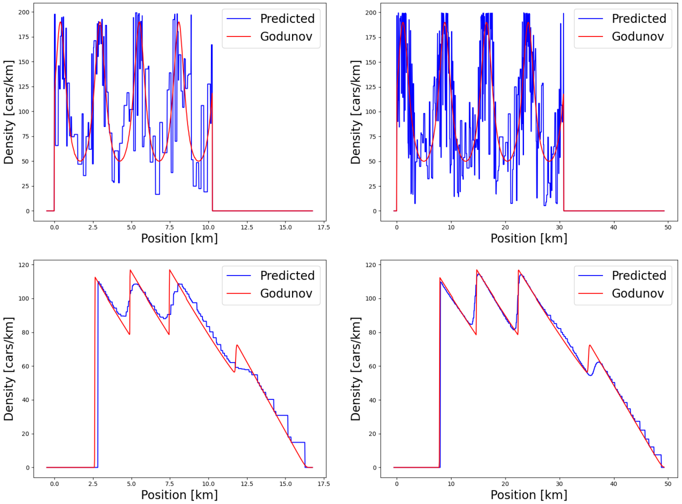

(a) $N = 1000$

(b) $N = 3000$

Comparison of reconstructed and macroscopic densities: **Top** Initial densities, **Bottom** Final densities

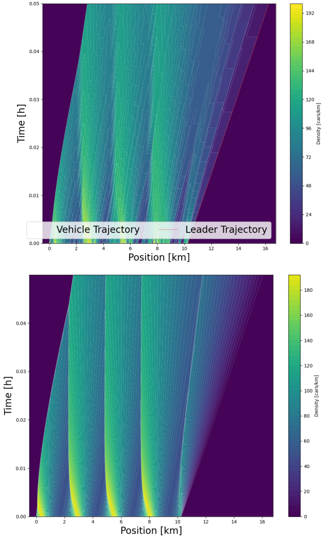

(a) $N = 1000$

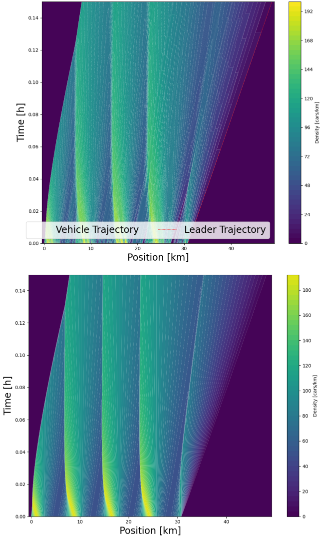

(b) $N = 3000$

Comparison of **reconstructed** and **macroscopic** densities: **Top** Reconstructed density, **Bottom** Godunov LWR density

Table of contents

Introduction

State-of-the art traffic flow models

(Learning-based) Optimization for traffic flow reconstruction

Numerical experiments

Conclusion and perspectives

Conclusion

Traffic state reconstruction approaches

- Model-based method
  $\Rightarrow$ uses microscopic and macroscopic models providing theoretical guarantees
  $\Rightarrow$ struggles to capture real-world complexities
- Data-driven method
  $\Rightarrow$ learns patterns directly from measurement data to predict near-future states
  $\Rightarrow$ requires extensive data for effectiveness
- Our approach
  $\Rightarrow$ **integrates physical priors with data observations**
  $\Rightarrow$ achieves reliable traffic reconstruction with limited observations

Perspectives

- Conservation law with unilateral constraint[6] (toll gate)

$$\begin{cases} \partial_t \rho(t,x) + \partial_x f(\rho(t,x)) = 0, & x \in \mathbb{R}, \quad t > 0, \\ \rho(0,x) = \bar{\rho}(x), & x \in \mathbb{R}, \\ f(\rho(t,0)) \leq q(t), & t > 0. \end{cases} \tag{20}$$

- Conservation law with moving bottleneck[7] (slow vehicle)

$$\begin{cases} \partial_t \rho(t,x) + \partial_x f(\rho(t,x)) = 0, & x \in \mathbb{R}, \quad t > 0, \\ \rho(0,x) = \bar{\rho}(x), & x \in \mathbb{R}, \\ f\left(\rho(t,y(t))\right) - \dot{y}(t)\rho(t,y(t)) \leq \frac{\alpha \rho_{\max}}{4 v_{\max}} \left(v_{\max} - \dot{y}(t)\right)^2, & t > 0, \\ \dot{y}(t) = \omega\left(\rho(t,y(t)_+)\right), & t > 0, \\ y(0) = y_0 \end{cases} \tag{21}$$

[6] Colombo and Goatin 2007.

[7] Delle Monache and Goatin 2014; Liard and Piccoli 2019.

Perspectives

- Network with a junction[8] J and N incoming roads and M outgoing ones

$$\begin{cases} \partial_t \rho_l(t,x) + \partial_x \left(f(\rho_l(t,x))\right) = 0, & t > 0, \quad x \in I_l, \quad l = 1, \ldots, N+M \\ \rho_l(0,x) = \rho_{0,l}(x), & x \in I_l = [a_l, b_l], \quad l = 1, \ldots, N+M \end{cases} \tag{22}$$

$$\Rightarrow \sum_{i=1}^{N} f\left(\rho_i(t,(b_i)_-)\right) = \sum_{j=N+1}^{N+M} f\left(\rho_j(t,(a_j)_+)\right) \text{ (Rankine Hugoniot)}$$

$$\Rightarrow \sum_{i=1}^{N} f\left(\rho_i(t,(b_i)_-)\right) \text{ is maximized}^{9} \text{ s.t. } f\left(\rho_j(\cdot,(a_j)_+)\right) = \sum_{i=1}^{N} a_{j,i} f\left(\rho_i(\cdot,(b_i)_-)\right)$$

- Investigate **limited-data reconstruction techniques for second-order** macroscopic models[10]

[8] Coclite, Piccoli, and Garavello 2005.
[9] Garavello and Piccoli 2006.
[10] Aw and Rascle 2000.

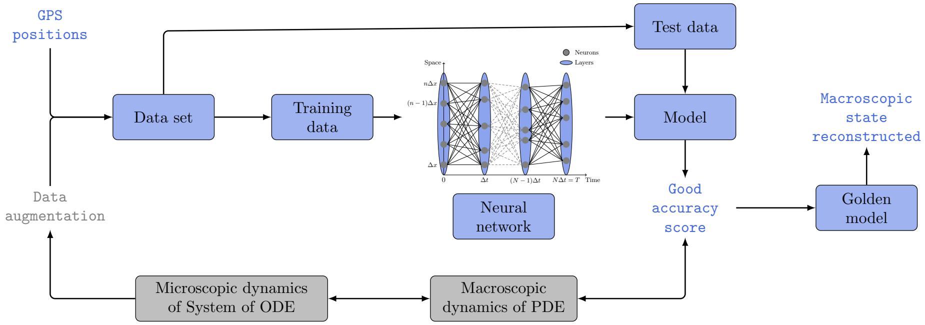

Traffic Flow Reconstruction Pipeline

To access the paper *Traffic Flow Reconstruction from Limited Collected Data* scan the QR code

References I

Aw, A. and M. Rascle (2000). "Resurrection of "second order" models of traffic flow". In: *SIAM Journal on Applied Mathematics* 60.3, pp. 916–938.

Barreau, M., M. Aguiar, J. Liu, and K. H. Johansson (2021). "Physics-Informed Learning for Identification and State Reconstruction of Traffic Density". In: *arXiv preprint arXiv:2103.13852.*

Coclite, G. M., B. Piccoli, and M. Garavello (2005). "Traffic Flow on a Road Network". In: *SIAM Journal on Mathematical Analysis* 36.6, pp. 1862–1886.

Colombo, R. M. and P. Goatin (2007). "A Well-Posed Conservation Law with a Variable Unilateral Constraint". In: *Journal of Differential Equations* 234.2, pp. 654–675.

Delle Monache, M. L. and P. Goatin (2014). "Scalar conservation laws with moving constraints arising in traffic flow modeling: An existence result". In: *Journal of Differential Equations* 257.8, pp. 4015–4040.

Di Francesco, M. and M. D. Rosini (2015). "Rigorous Derivation of Nonlinear Scalar Conservation Laws from Follow-the-Leader Type Models via Many Particle Limit". In: *arXiv preprint arXiv:1404.7062.*

Garavello, M. and B. Piccoli (2006). *Traffic Flow on Networks*. Vol. 1. Applied Mathematics. American Institute of Mathematical Sciences.

Holden, H. and N. H. Risebro (2017). "The Continuum Limit of Follow-the-Leader Models: A Short Proof". In: *arXiv preprint arXiv:1709.07661.*

Liard, T. and B. Piccoli (2019). "Well-posedness for scalar conservation laws with moving flux constraints". In: *SIAM Journal on Applied Mathematics* 79.2, pp. 641–667.

References II

Liu, J., M. Barreau, M. Cicic, and K. H. Johansson (2020). “Learning-Based Traffic State Reconstruction Using Probe Vehicles”. In: *arXiv preprint arXiv:2011.05031*.

Learning method

- Dataset consists of **artificial data** based on simulated (classical) FtL dynamics (3)
- Sampling of PVs yielding a **balanced representation** of overall traffic
- **Neural network** architecture designed to **understand dynamics of traffic**
- Residual network (ResNet) where each block corresponds to a single time step
- Input $\bar{x}$ and state $x(.)$ is propagated by mirroring Euler discretization

$$x(t+\Delta t) = x(t) + V(Wx(t)+b)\Delta t \tag{23}$$

- Weights and biases W, b are functions of α

$$\begin{cases} W_{i,i} := -\frac{N}{\alpha_i L}, & i = 0, \dots, n-1, \\ W_{i,i+1} := \frac{N}{\alpha_i L}, & i = 1, \dots, n-2, \\ W_{i,j} := 0, & \text{otherwise}, \end{cases} \quad b_i(t) =:= \delta_{i,n} \frac{N}{\alpha_i L}\left(v_{\max} t + \bar{x}_n^N\right), \quad t \in [0, T] \tag{24}$$

- Nonlinear dynamic map V acts as physics grounded activation function
- Backpropagation to minimize predictions errors $\mathcal{L}^{\text{train}}(x(T), \bar{y}) = \frac{1}{n}\sum_{j=0}^{n} |x_j^\alpha(T) - \bar{y}_j^N|^2$

Well-posedness

Lemma (Discrete maximum principle)

For solution $x(t)$ of (7) with v satisfying (10a)-(10c), for all $i = 0, \cdots, n-1$,

$$\frac{\alpha_i^N L}{NM} \leq x_{i+1}^N(t) - x_i^N(t) \leq \bar{x}_n^N - \bar{x}_0^N + (v_{\max} - v(M))\, t, \quad \forall t \in [0, T], \tag{25}$$

where $M := \max_i \left(\frac{\alpha_i^N L}{N(\bar{x}_{i+1}^N - \bar{x}_i^N)} \right)$

Sketch of proof

- Lower bound is satisfied at $t = 0$, aim at extending property for all times up to T
- Equivalent to show

$$\inf_{0<t\leq T} [x_{i+1}(t) - x_i(t)] \geq \frac{\alpha_i^N L}{NM}, \quad i = 0, \dots, n-1. \tag{26}$$

$\Rightarrow$ **recursive argument** (backward from $n-1$ to 0)

- Property is true for $i = n-1$

$$\begin{aligned} x_n(t) - x_{n-1}(t) =& \bar{x}_n - \bar{x}_{n-1} + \int_0^t \left(v_{\max} - v\left(\frac{\alpha_n^N L}{N(x_n(s) - x_{n-1}(s))} \right) \right) ds \\ \geq& \bar{x}_n - \bar{x}_{n-1} \geq \frac{\alpha_{n-1}^N L}{NM}. \end{aligned}$$

- Assume property is verified for $j+1$ and prove it is still satisfied for j

$$\inf_{0<t\leq T} [x_{j+2}(t) - x_{j+1}(t)] \geq \frac{\alpha_{j+1}^N L}{NM}. \tag{27}$$

Sketch of proof

- By contradiction, assume that there exists $0 \le t_1 < t_2$ such that

$$\begin{cases} x_{j+1}(t) - x_j(t) \ge \frac{\alpha_j^N L}{NM}, & t < t_1 \\ x_{j+1}(t) - x_j(t) = \frac{\alpha_j^N L}{NM}, & t = t_1 \\ x_{j+1}(t) - x_j(t) < \frac{\alpha_j^N L}{NM}, & t_1 < t \le t_2. \end{cases} \tag{28}$$

- Since v is decreasing

$$\begin{aligned} x_j(t) =& x_j(t_1) + \int_{t_1}^{t} v\left(\frac{\alpha_j^N L}{N(x_{j+1}(s) - x_j(s))}\right) ds \\ \le& x_j(t_1) + v\left(M\right)\left(t - t_1\right), \end{aligned}$$

- Moreover from (27), for $t_1 < t \le t_2$,

$$x_{j+1}(t) = x_{j+1}(t_1) + \int_{t_1}^{t} v\left(\frac{\alpha_{j+1}^N L}{N(x_{j+2}(s) - x_{j+1}(s))}\right) ds \ge x_{j+1}(t_1) + v\left(M\right)\left(t - t_1\right)$$

$$\Rightarrow x_{j+1}(t) - x_j(t) \ge x_{j+1}(t_1) - x_j(t_1) = \frac{\alpha_j^N L}{NM}$$

which contradicts (28), so that (26) is satisfied

Sketch of proof

- Show upper bound for $i = 0, \dots, n-1$ and $t \in [0, T]$
- Recalling assumptions on v and applying system's dynamics

$$
\begin{aligned}
x_{i+1}(t) - x_i(t) &= x_{i+1}(0) - x_i(0) + \int_0^t \left(\dot{x}_{i+1}(s) - \dot{x}_i(s)\right) ds \\
&\leq \bar{x}_{i+1} - \bar{x}_i + \int_0^t \left(v_{\max} - v\left(\frac{\alpha_i^N L}{N(x_{i+1}(s) - x_i(s))} \right) \right) ds \\
&\leq \bar{x}_n - \bar{x}_0 + \left(v_{\max} - v(M)\right) t,
\end{aligned}
$$

- Last equality is obtained from lower bound $\Rightarrow$ proof is complete

Outline of convergence analysis

- Prove that ρ^N predicted by ML converges to solution of LWR (4) when the $N \to \infty$
- Main challenge is imposing a condition on distribution of α which would guarantee convergence
- Demonstrate that $\rho^N(0,\cdot)$ converges to $\bar{\rho}$ in LWR (4)
- Consider empirical discrete density

$$\widehat{\rho}^N(t,\cdot) := \frac{L}{N}\sum_{i=0}^{n-1} \alpha_i^N \delta_{x_i(t)}(\cdot), \quad t \in [0,T]. \tag{29}$$

- **Important observation**: by construction, initial traffic density must satisfy

$$\bar{x}_{i+1} = \sup\left\{x \in \mathbb{R} : \int_{\bar{x}_i}^{x} \bar{\rho}(y)dy \leq \frac{\alpha_i L}{N}\right\}, \quad i = 0,\dots,n-1 \tag{30}$$

$\Rightarrow$ although no access to ground-truth initial car density $\bar{\rho}$, initial positions $\bar{x}_i$ verify (30)

Theorem Convergence of approximate density to solution of LWR

Under some assumptions, piecewise-constant density

$$\rho^N(t,x) = \sum_{i=0}^{n-1} \frac{\bar{\alpha}_i^N L}{N(x_{i+1}^N(t) - x_i^N(t))} \chi_{[x_i^N(t), x_{i+1}^N(t))}(x), \quad x \in \mathbb{R}, \quad t \in [0,T], \tag{31}$$

where $\bar{\alpha}_i^N \in \mathcal{A}^N$ is a solution to (13) converges to **unique entropy** solution ρ of

$$\begin{cases} \dfrac{\partial}{\partial t}\rho(t,x) + \dfrac{\partial}{\partial x} f(\rho(t,x)) = 0, \quad x \in \mathbb{R}, \quad t \in [0,T], \\ \rho(0,x) = \bar{\rho}(x), \quad x \in \mathbb{R} \end{cases} \tag{32}$$

Sketch of proof

- Ensures discretization aligns consistently with true initial density when $N \to \infty$
- Notations: for $t \in [0, T]$, $\rho(t) := \rho(t, \cdot)$ and $\widehat{\rho}(t) := \widehat{\rho}(t, \cdot)$
  In particular, at $t = 0$, $\rho(0) := \rho(0, \cdot)$ and $\widehat{\rho}(0) := \widehat{\rho}(0, \cdot)$
- Use **Wasserstein distance** defined in Di Francesco and Rosini 2015 by

$$\mathrm{W}_{L,1}(f, g) = \|f(]-\infty, \cdot]) - g(]-\infty, \cdot]\|_{L^1(\mathbb{R},\mathbb{R})} \tag{33}$$

Proposition

Let $\bar{\rho}$ satisfy (30) and assume that

$$\max_{i=0,\dots,n-1} \alpha_i^N = o(N) \tag{34}$$

Then $(\rho^N(0))_{n\in\mathbb{N}}$ and $(\widehat{\rho}^N(0))_{n\in\mathbb{N}}$ converge to $\bar{\rho}$ in the sense of the $\mathrm{W}_{L,1}$ -Wasserstein distance in (33)

Remark

A particular case of assumption (34) is when $\max_{i=0,\dots,n-1} \alpha_i^N \leq \frac{CN}{\log(N)}$ for some $C > 0$

Sketch of proof

- Using $l_N := L/N$, $\mathrm{W}_{L,1}$- distance and discrete density in (8)

$$\begin{aligned} \mathrm{W}_{L,1}(\rho^N(0),\widehat{\rho}^N(0)) &= \sum_{i=0}^{n-1}\int_{\bar{x}_i}^{\bar{x}_{i+1}^N}\left(\alpha_i^N l_N - \rho_i^N(t)\,(x-\bar{x}_i)\right)dx \\ &= \sum_{i=0}^{n-1}\alpha_i^N l_N\int_{\bar{x}_i}^{\bar{x}_{i+1}}\left(1-\frac{x-\bar{x}_i}{\bar{x}_{i+1}-\bar{x}_i}\right)dx \\ &\le \max_{i=0,\dots,n}\{\alpha_i^N\} l_N\,(\bar{x}_n-\bar{x}_0) \end{aligned} \tag{35}$$

$\Rightarrow$ it suffices to prove that $(\widehat{\rho}^N(0))_{n\in\mathbb{N}}$ converges to $\bar{\rho}$ in sense of $\mathrm{W}_{L,1}$- distance

- Using expressions of both Euler (9) and empirical (29) discrete densities

$$\begin{aligned} &\mathrm{W}_{L,1}(\widehat{\rho}^N(0),\bar{\rho}) \\ &= \sum_{i=0}^{n-2}\int_{\bar{x}_i}^{\bar{x}_{i+1}}\left(\left(\sum_{j=0}^{i-1}\alpha_j^N l_N - \int_{\bar{x}_0}^{\bar{x}_i}\bar{\rho}(y)dy\right)+\left(\alpha_i^N l_N - \int_{\bar{x}_i}^{x}\bar{\rho}(y)dy\right)\right)dx \\ &\quad + \int_{\bar{x}_{n-1}}^{\bar{x}_n}\left(\sum_{j=0}^{n-2}\alpha_j^N l_N - \int_{\bar{x}_0}^{\bar{x}_{n-1}}\bar{\rho}(y)dy\right)+\left(\alpha_{n-1}^N l_N - \int_{\bar{x}_{n-1}}^{x}\bar{\rho}(y)dy\right)dx \end{aligned}$$

Sketch of proof

- From atomization of initial density (30)

$$
\begin{aligned}
&\mathrm{W}_{L,1}(\widehat{\rho}^N(0), \bar{\rho}) \\
&\leq \sum_{i=0}^{n-2} \int_{\bar{x}_i}^{\bar{x}_{i+1}} \left(\alpha_i^N l_N - \int_{\bar{x}_i}^{x} \bar{\rho}(y) dy \right) dx + \int_{\bar{x}_{n-1}}^{\bar{x}_n} \left(\alpha_{n-1}^N l_N - \int_{\bar{x}_{n-1}}^{x} \bar{\rho}(y) dy \right) dx \\
&= \sum_{i=0}^{n-1} \alpha_i^N l_N \int_{\bar{x}_i}^{\bar{x}_{i+1}} \left(1 - \frac{1}{\alpha_i^N l_N} \int_{\bar{x}_i}^{x} \bar{\rho}(y) dy \right) dx \\
&\leq \max_{i=0,\dots,n} \left\{ \alpha_i^N \right\} l_N (\bar{x}_n - \bar{x}_0)
\end{aligned}
$$

- From (34)-(35), conclude that $(\rho^N(0))_{n\in\mathbb{N}}$ converges to $\bar{\rho}$ in sense of $\mathrm{W}_{L,1}$-Wasserstein distance
- Finally generalize convergence to unique entropy solution of conservation law (4)
  $\Rightarrow$ require only minor modifications to arguments in Di Francesco and Rosini 2015, Theorem 3

Rarefaction wave scenario

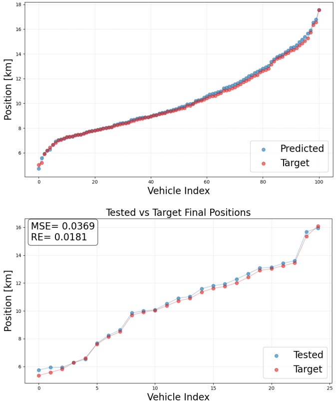

(a) $N = 1000$

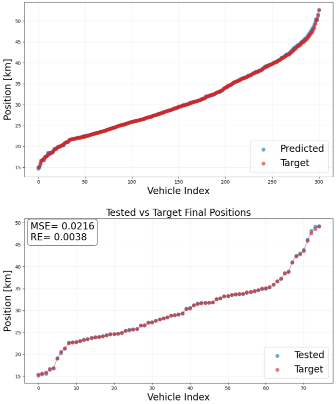

(b) $N = 3000$

Comparison of predicted and target final PV positions: **Top** Results from **training** procedure, **Bottom** Results on **test** sounds

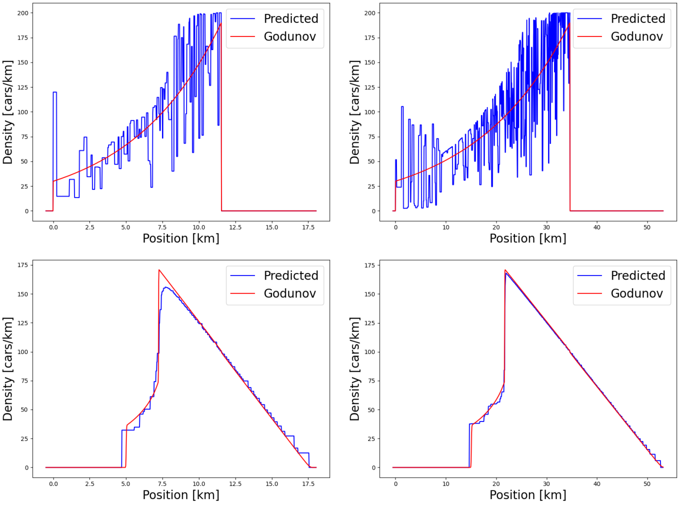

(a) $N = 1000$

(b) $N = 3000$

Comparison of reconstructed and macroscopic densities: **Top** Initial densities, **Bottom** Final densities

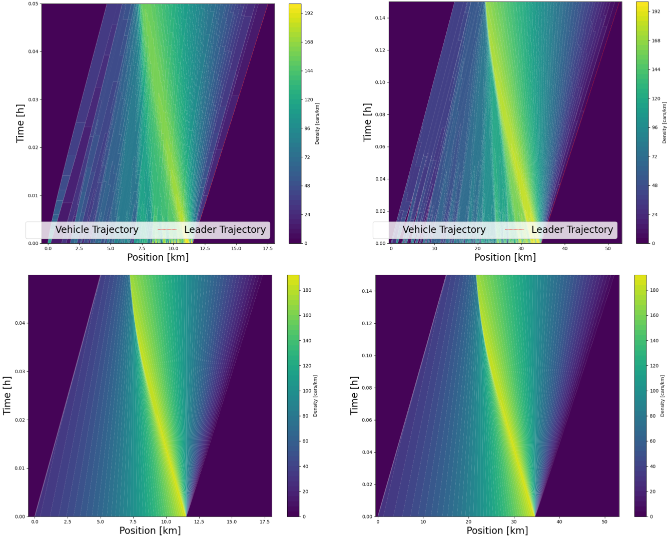

(a) $N = 1000$ (b) $N = 3000$

Comparison of **reconstructed** and **macroscopic** densities: **Top** Reconstructed density, **Bottom** Godunov LWR density

Shock wave scenario

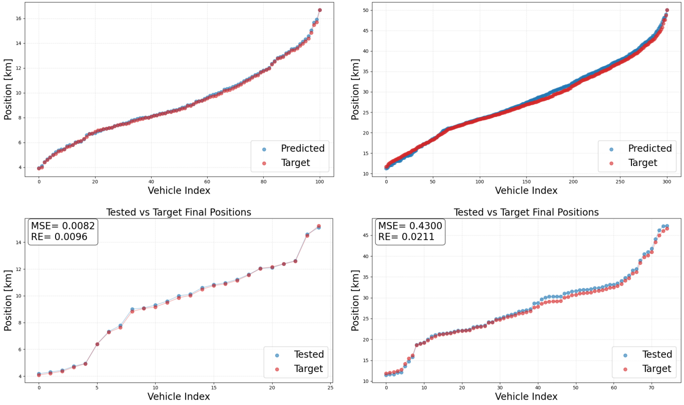

(a) $N = 1000$ (b) $N = 3000$

Comparison of predicted and target final PV positions: **Top** Results from **training** procedure, **Bottom** Results on **test** sounds

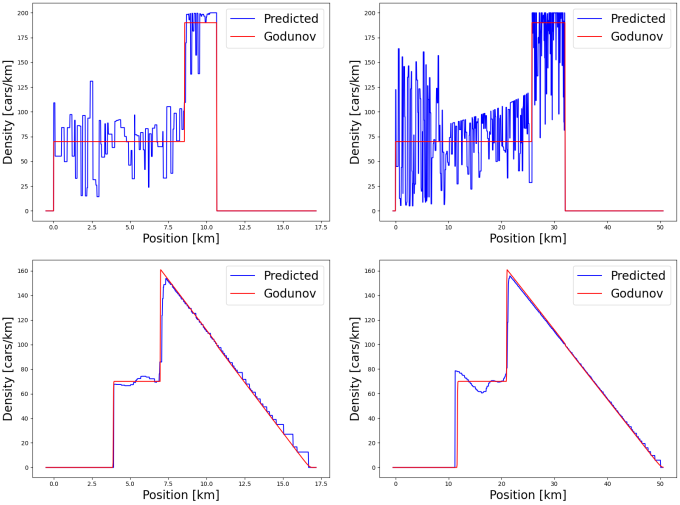

(a) $N = 1000$ (b) $N = 3000$

Comparison of reconstructed and macroscopic densities: **Top** Initial densities, **Bottom** Final densities

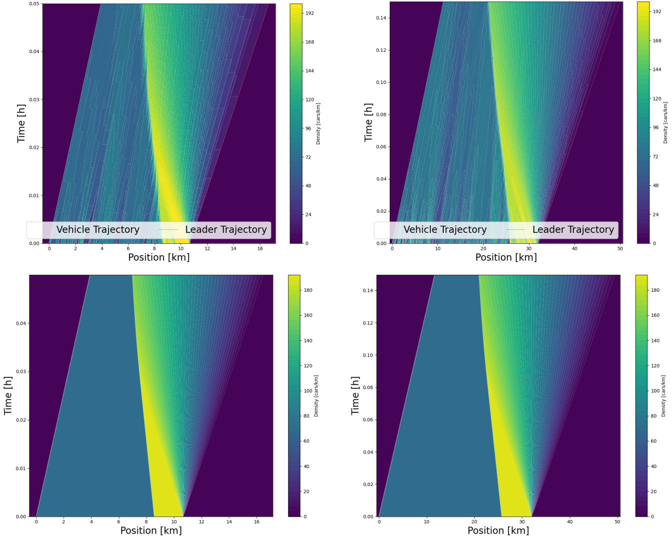

(a) $N = 1000$ (b) $N = 3000$

Comparison of **reconstructed** and **macroscopic** densities: **Top** Reconstructed density, **Bottom** Godunov LWR density